Structure
Article

Inhibition versus Potentiation of Ligand-Gated Ion Channels Can Be Altered by a Single Mutation that Moves Ligands between Intra- and Intersubunit Sites

Torben Brömstrup,[1,2] Rebecca J. Howard,[3] James R. Trudell,[4] R. Adron Harris,[5] and Erik Lindahl[1,2,*]
[1]Science for Life Laboratory, KTH Royal Institute of Technology & Stockholm University, 17121 Solna, Sweden
[2]Center for Biomembrane Research, Department of Biochemistry & Biophysics, Stockholm University, 10691 Stockholm, Sweden
[3]Department of Chemistry, Skidmore College, Saratoga Springs, NY 12866, USA
[4]Department of Anesthesia and Beckman Program for Molecular and Genetic Medicine, Stanford University School of Medicine, Stanford, CA 94305, USA
[5]Waggoner Center for Alcohol and Addiction Research, University of Texas at Austin, Austin, TX 78712, USA
*Correspondence: erik.lindahl@scilifelab.se
http://dx.doi.org/10.1016/j.str.2013.06.018

SUMMARY

Pentameric ligand-gated ion channels (pLGICs) are similar in structure but either inhibited or potentiated by alcohols and anesthetics. This dual modulation has previously not been understood, but the determination of X-ray structures of prokaryotic GLIC provides an ideal model system. Here, we show that a single-site mutation at the F14′ site in the GLIC transmembrane domain turns desflurane and chloroform from inhibitors to potentiators, and that this is explained by competing allosteric sites. The F14′A mutation opens an intersubunit site lined by N239 (15′), I240 (16′), and Y263. Free energy calculations confirm this site is the preferred binding location for desflurane and chloroform in GLIC F14′A. In contrast, both anesthetics prefer an intrasubunit site in wild-type GLIC. Modulation is therefore the net effect of competitive binding between the intersubunit potentiating site and an intrasubunit inhibitory site. This provides direct evidence for a dual-site model of allosteric regulation of pLGICs.

INTRODUCTION

Despite their widespread use in surgery for more than 150 years, the molecular action of volatile anesthetics is poorly understood. Early theories of nonspecific action on cell membranes have given way to evidence for direct modulation of membrane proteins, including the family of pentameric ligand-gated ion channels (pLGICs; Miller, 2002; Urban and Bleckwenn, 2002). In this family, pharmacologically relevant concentrations of volatile anesthetics potentiate function of most $GABA_A$ receptors ($GABA_ARs$) and glycine receptors (GlyRs), while they inhibit most nicotinic acetylcholine receptors (nAChRs; Forman and Miller, 2011). The sites of action of volatile anesthetics on pLGICs are usually allosteric; they are believed to be distal to the site(s) of agonist binding, and for most channels it is not possible for the allosteric ligand to open the channel without the agonist present (Cascio, 2006). This remarkable diversity in the action of allosteric ligands in a single family of receptors is different. It provides an interesting opportunity to better understand membrane protein conformational changes and allosteric modulation in general, as well as mechanisms of action for how volatile anesthetics and alcohol perturb the function of ligand-gated ion channels in particular. For a recent review, see Corringer et al., 2012.

Because there are still no X-ray structures available for the $GABA_ARs$ and GlyRs, and only a lower-resolution cryo-electron microscopy structure exists for the nAChR (Unwin, 2005), some of the historically most important studies of pLGICs have used site-directed mutagenesis combined with photolabeling or electrophysiology to experimentally characterize the modulation sites for alcohols and anesthetics. Early photolabeling studies (Pedersen and Cohen, 1990) proposed a binding site between subunits for nAChRs, and more recent work has shown that the modulation of nAChR is influenced by a diverse range of binding sites, including a site in the extracellular domain (Ziebell et al., 2004) and two sites in the channel (Chiara et al., 2009; Pandhare et al., 2012) for charged ligands, while uncharged ligands might bind between subunits close to the extracellular end of the M2 helix (Arevalo et al., 2005; Chiara et al., 2003). Time-resolved photolabeling studies have further identified state-dependent binding sites in the transmembrane (TM) domain and shown that agonist-driven channel opening can enhance anesthetic binding to a hydrophobic binding site, which could point to a selected fit model (Arevalo et al., 2005). There is also evidence for slow and fast desensitization of the channels being linked to separate conformational changes in two different cavities (Yamodo et al., 2010). Some of the first evidence for specific action sites of alcohol and volatile anesthetics on heteromeric GABA was provided by Mihic and colleagues (Mihic et al., 1997), using chimeric receptor constructs with α_1/β_2 subunits to identify α_1S270/β_2N265 (15′ M2) and α_1A291/β_2M286 as critical for modulation. Photolabeling studies on GABA with etomidate analogs (Chiara et al., 2012; Li et al., 2006) have identified intersubunit binding of etomidate close to α_1S270/β_2N265 (M2 15′), and early simulations of homology models of GlyR could keep ethanol stable in an intersubunit site formed by S267, A288, and I229 (Cheng et al., 2008). However, other

data suggest that the anesthetic propofol binds close to the extracellular end of the M3 segment in GABA, and, at least for GlyR, there are functional mutation studies indicating independent contributions of S267 (M2 15′) and A52 in the extracellular domain loop 2 (Brejc et al., 2001), which suggests there might be multiple potentiating binding sites (Crawford et al., 2007; Mascia et al., 2000; Perkins et al., 2010).

Because no high-resolution structure has yet been determined for a human pLGIC, substantial insight has emerged from the structures of closely related prokaryotic proteins such as the *Gloeobacter violaceus* ligand-gated ion channel (GLIC; Bocquet et al., 2009; Hilf et al., 2010). This bacterial homolog shares 20% amino acid identity with the human α7 nAChR (Bocquet et al., 2007) and exhibits inhibition by volatile anesthetics, similar to nAChRs (Weng et al., 2010). GLIC has been an important template for homology models of human receptors, and in previous work, we have reported microsecond simulations of GlyR where ethanol spontaneously diffuses to and binds in an intersubunit location (Murail et al., 2011). This would appear to be contradicted by GLIC co-crystals with the anesthetics desflurane and propofol located in an intrasubunit site (Nury et al., 2011), but the recent structure of the eukaryotic GluCl channel by Hibbs and colleagues has the ligand ivermectin bound between subunits (Hibbs and Gouaux, 2011) in close contact with S260 (M2 15′), A261, and G262. Superficially, all these data on different receptors might seem incompatible, although another option is the existence of multiple different binding sites for alcohols and/or anesthetics (Bali and Akabas, 2004; Ernst et al., 2005; Jansen and Akabas, 2006; Trudell and Bertaccini, 2004).

While the GLIC X-ray structures (Nury et al., 2011) point to an intrasubunit binding site, this prokaryotic channel is mostly inhibited by volatile anesthetics such as desflurane, propofol, or chloroform, as well as long chain n-alcohols in contrast to many of its eukaryotic homologs. This result makes it harder to say anything specific about the potentiating allosteric site and mechanism of pLGICs in general. However, recent mutagenesis studies of GLIC have opened new possibilities to use this channel as a model system for allosteric potentiation. Replacing the TM domain of GLIC by the α1 subunit from GlyR reverses modulation of GLIC by anesthetics and long-chain alcohols from inhibitory to potentiating (Duret et al., 2011), supporting this domain's role in mediating inhibition and potentiation. In fact, alcohols as large as *n*-hexanol can be converted from inhibitors to potentiators through a single point mutation, F238A, in the second TM helix (M2) of GLIC (Howard et al., 2011a). This mutation converts GLIC into a highly ethanol-sensitive channel comparable to its eukaryotic relatives GlyRs and GABA. Molecular dynamics (MD) simulations indicated this is caused by the opening of a cavity at the intersubunit interface that may mediate potentiation, without substantially altering the intrasubunit binding cavity observed in X-ray structures. We believe these changes cannot be explained from a single anesthetic or alcohol-binding site in pLGICs, no matter what the location is, but that it requires a dual action mechanism for channel inhibition and potentiation. Indeed, microsecond simulations of GLIC F238A in the presence of ethanol show enhanced intersubunit density of ethanol (Murail et al., 2012), which would correlate well with the proposed binding sites for anesthetics and alcohols in eukaryotic channels (Bertaccini et al., 2005; Cheng et al., 2008; Forman and Miller, 2011).

Recent efforts to simulate anesthetic binding to GLIC using MD (Brannigan et al., 2010) or combined modeling and tryptophan quenching (Chen et al., 2010) have suggested binding to both intrasubunit and intersubunit sites, as well as sites in the pore and in loop regions of TM domains. One approach to distinguish between such promiscuous possibilities is to calculate the free energies of binding of a computationally docked compound in various putative binding sites (Foloppe and Hubbard, 2006), an approach that is becoming increasingly accessible to membrane protein studies (LeBard et al., 2012; Lindahl and Sansom, 2008). In particular, quantitative data on the contributions of specific sites to anesthetic binding can be compared directly to experiments to connect functional and molecular-level data and critically test different models for modulation.

In this study, we provide evidence for a dual-site allosteric modulation effect on ligand-gated ion channels, where the intrasubunit site is inhibitory and the intersubunit site potentiating. This has been achieved by combining electrophysiology with MD simulations to probe how the F238A mutation changes the modulation response of GLIC to volatile anesthetics. The single-site mutation not only shifts, but also completely reverses the modulation effect in experiments and causes GLIC to be potentiated rather than inhibited by desflurane and chloroform. By using docking to a range of putative sites as well as free energy calculations, we show this is explained by the presence of two binding sites, where the intrasubunit site has the best affinity for both compounds in wild-type (WT) GLIC, but in the F238A mutant, the affinity is swapped with the anesthetics preferring intersubunit binding. This provides direct support for an action model where desflurane and chloroform primarily bind intrasubunit in WT GLIC and inhibit the channel, while the F238A mutant has a potentiating binding site between subunits.

RESULTS

GLIC WT and F238A Channels Are Differentially Modulated by Volatile Anesthetics

Whereas GLIC exhibits inhibition by long-chain alcohols such as *n*-hexanol, the single-site mutant F238A exhibits potentiation by the same agents (Howard et al., 2011a). Given past evidence that alcohols and volatile anesthetics may act via shared binding sites on pLGICs (Mascia et al., 2000), we investigated the modulation of GLIC by a variety of volatile anesthetics. We measured anesthetic modulation by two-electrode voltage clamp electrophysiology in *Xenopus laevis* oocytes of GLIC currents at 10% maximal proton activation, using a similar protocol to that previously described for *n*-alcohols (Howard et al., 2011a). Pharmacologically relevant doses of volatile anesthetics are generally described by the minimum alveolar concentration (MAC) required to eliminate response to a noxious stimulus in 50% of subjects (Sonner et al., 2003). The volatile agents desflurane, chloroform, enflurane, and isoflurane inhibited the function of WT GLIC at or below three times MAC (Weng et al., 2010), while they potentiated the function of GLIC mutant F238A (Figure 1A).

To quantify the differential modulation of GLIC WT and F238A channels, we measured modulation at a range of concentrations of desflurane, an inhalational agent commonly used for general anesthesia (Meyer, 2010) that was recently co-crystallized in a TM intrasubunit site of GLIC (Nury et al., 2011). WT GLIC was

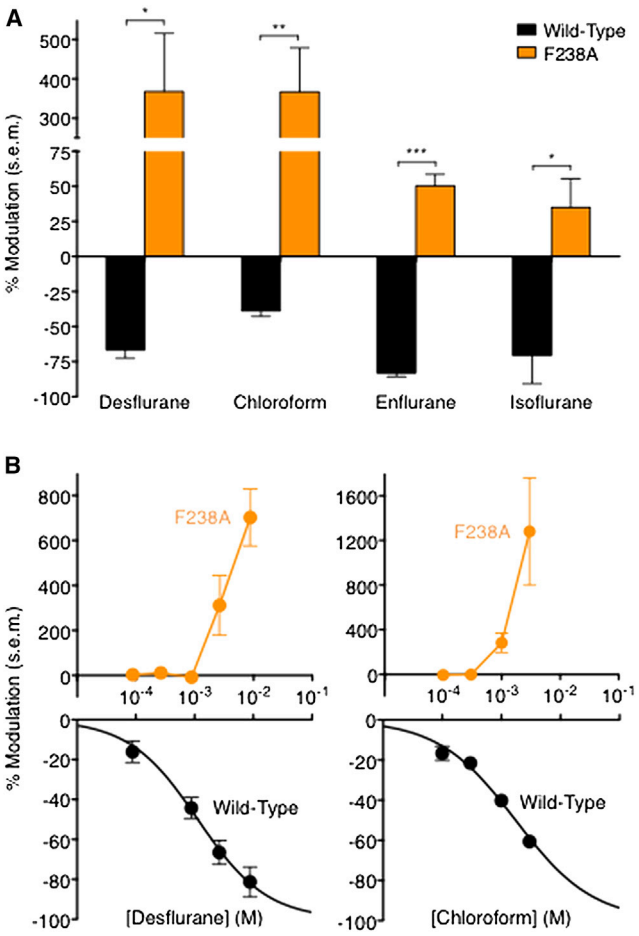

Figure 1. Enhancement of GLIC Potentiation in the F238A Mutant

(A) Modulation of GLIC WT (black) and F238A (orange) channels by volatile anesthetics: 1.00 mM chloroform, 2.64 mM desflurane, 1.68 mM enflurane, and 0.90 mM isoflurane (significance versus WT, unpaired t test, *$p < 0.05$; **$p < 0.01$; ***$p < 0.001$.) The vertical axis is broken to display both WT and mutant responses clearly. Error bars are SEM; n = 3–10.

(B) Concentration-dependent modulation of GLIC WT (black, lower panel) and F238A (orange, upper panel) channels by desflurane. Black curve represents nonlinear regression fit of WT data; orange lines connect F238A mutant data points, which were poorly fit by regression analysis. Positive and negative vertical axes are scaled independently to display WT and mutant responses clearly. Error bars are SEM; n = 3–14.

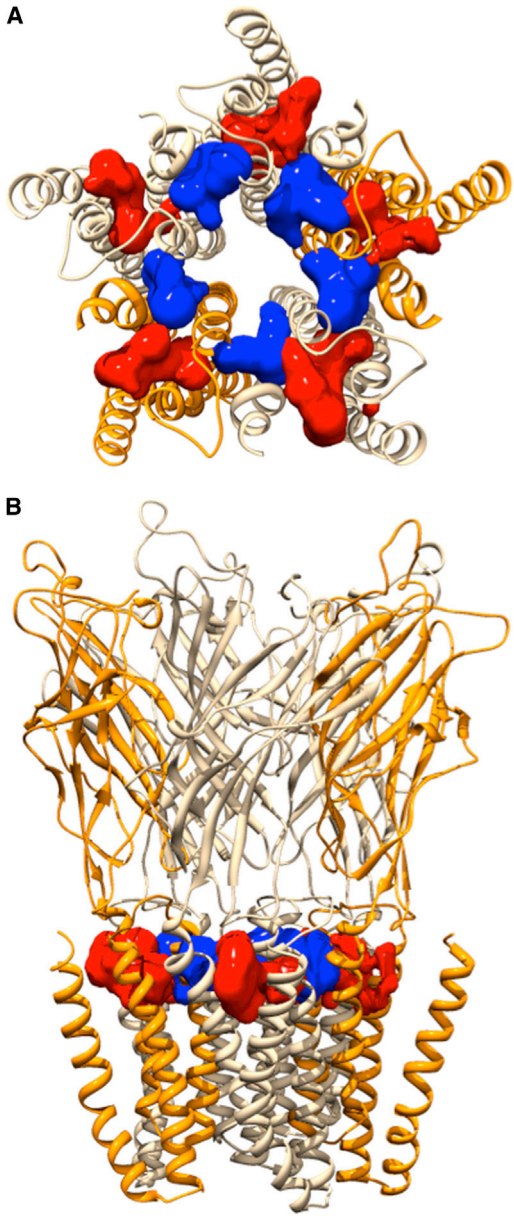

Figure 2. GLIC F238A TM Cavities

(A and B) Illustration of the intrasubunit (red) and intersubunit (blue) cavities after equilibration of GLIC F238A, shown from the extracellular side (A) and in the membrane plane (B). The five subunits are rendered in slightly different colors to depict the cavity locations. Cavities were calculated and illustrated using the Surfnet module (Laskowski, 1995) in the Chimera program (Pettersen et al., 2004).

inhibited by desflurane in a concentration-dependent manner with a half-maximal concentration (IC_{50}) of 1.1 mM, ~1.3 MAC ($LogIC_{50}$ −2.9 ± 0.087), and a Hill coefficient less than 1 (0.74 ± 0.19; Figure 1B, black). Conversely, GLIC F238A exhibited little or no modulation up to 1 MAC desflurane, but was enhanced more than 4-fold by higher concentrations (Figure 1B, orange). GLIC potentiation did not appear to saturate at the highest concentration tolerated by oocytes.

Structural Details of Intrasubunit and Intersubunit Binding

To identify the binding differences between GLIC WT and F238A, we needed to find the best binding poses in the intersubunit and intrasubunit cavities (Figure 2). We applied ligand docking to obtain initial binding sites followed by 20 ns unrestrained MD to identify multiple kinetically distinct binding poses. These poses were used to obtain binding affinities of both anesthetics in the two sites site of WT and F238A GLIC. The binding free energy was calculated independently for each pose, and an occupancy-weighted average calculated in each site. To increase sampling in the simulations, desflurane or chloroform ligands were placed in identical poses in each of the subunit sites

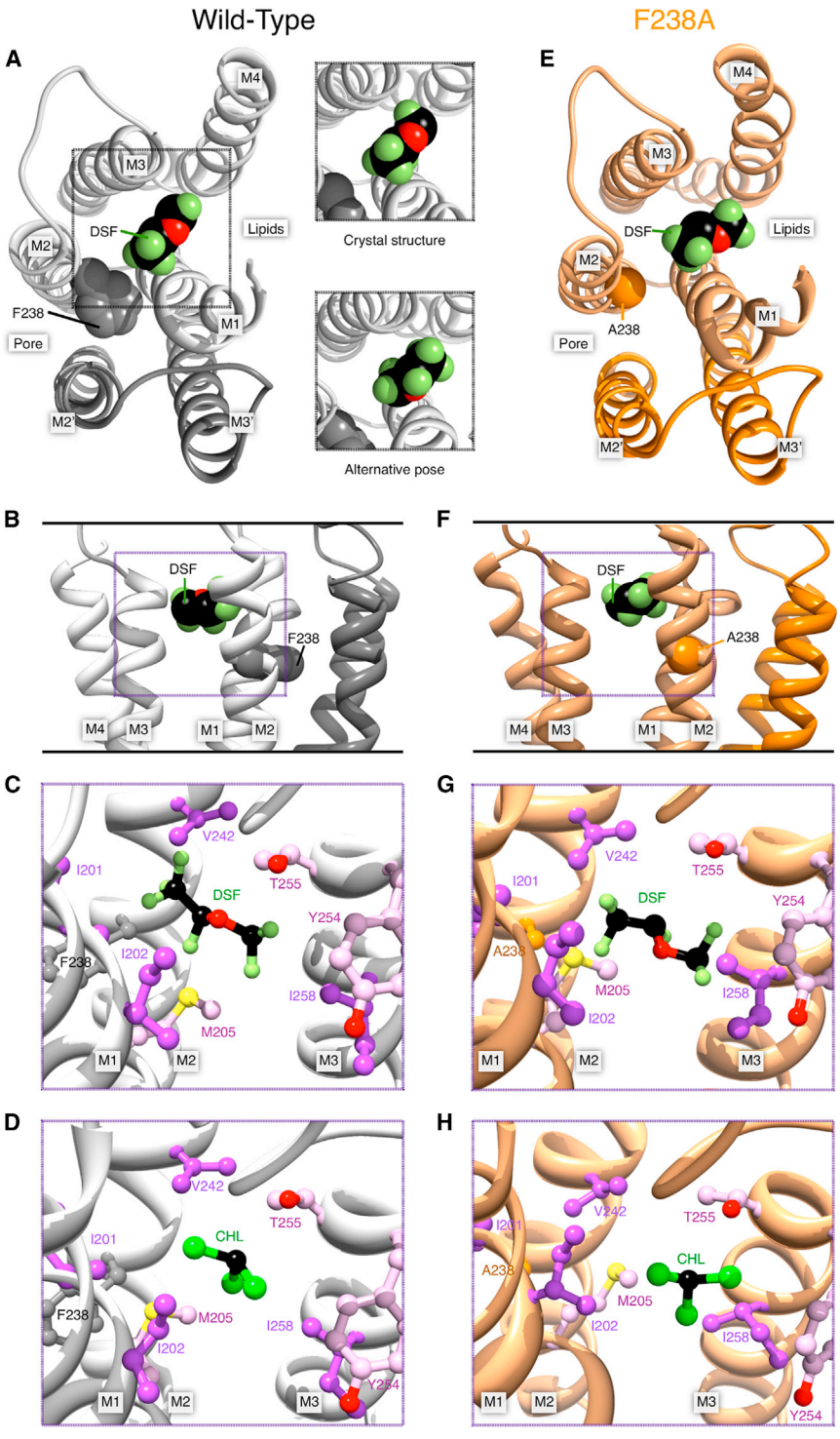

Figure 3. Desflurane and Chloroform Poses in the Intrasubunit Cavity of GLIC

(A) Left, desflurane in the intrasubunit binding site, viewed from the extracellular side. For clarity, only the TM helices M1–M4 of the proximal subunit (light gray) and M2–M3 the distal subunit (dark gray) are shown. Residue F238 (spheres) and helices contributing to the intrasubunit cavity are labeled. Right, equivalent view from the extracellular side and a second kinetically distinct pose.

(B) Desflurane binding in WT viewed in the plane of the membrane in the pore, with F238 marked.

(C and D) Other important residues surrounding the binding site after equilibration (C), and residue environment with chloroform (CHL) bound (D).

(E–H) Equivalent binding conformations in the F238A mutant, with residue F238A marked. Overall, the intrasubunit binding was largely unaffected by the mutation.

See also Figures S1, S2, and Table S1.

(Figure 2), although this is not strictly required for modulation in experiments (Mowrey et al., 2013).

Intrasubunit Binding Conformations

Desflurane was docked into GLIC WT and F238A by using the cavity from the experimentally identified binding site (Nury et al., 2011). Neither root-mean-square deviation (rmsd) calculation nor manual inspection indicated any significant differences in the set of binding poses between the two structures (Figure S1 available online), which is reasonable because the mutation did not directly affect this site. The interaction site of desflurane in the docking-derived intrasubunit site was made up by I201, I202, and S205 (I206) of helix M1, V242 of M2, and T255, Y254, and I258 (I259) of M3, which is identical to the interacting residues observed in the X-ray co-crystal reported earlier (Nury et al., 2011).

Representative conformations of desflurane obtained by clustering of snapshots along the trajectories, as well as visual inspection of the trajectories, indicated two poses (Figure 3A). The conformational diversity and relatively high mobility of desflurane in the intrasubunit cavity (root-mean-square fluctuation [rmsf] of 3.55 Å in WT and 2.96 Å in F238A) makes it difficult to compare with a limited-resolution electron density. However, we found the representative conformation of one cluster to be within 0.6 Å rmsd of the crystal structure (Nury et al., 2011), which indicates some agreement between simulations and crystallographic data. The crystal structure points toward hydrogen bond formation between T255 and the oxygen atom of desflurane. However, while analysis of the trajectories shows that the mere distance between the oxygen of desflurane and the hydroxyl group of T255 might be compatible with hydrogen bonding, the geometric constraints for hydrogen bond formation are rarely fulfilled either in WT GLIC or the F238A mutant. The large mobility of desflurane suggests its binding in the intrasubunit site might not be due specifically to

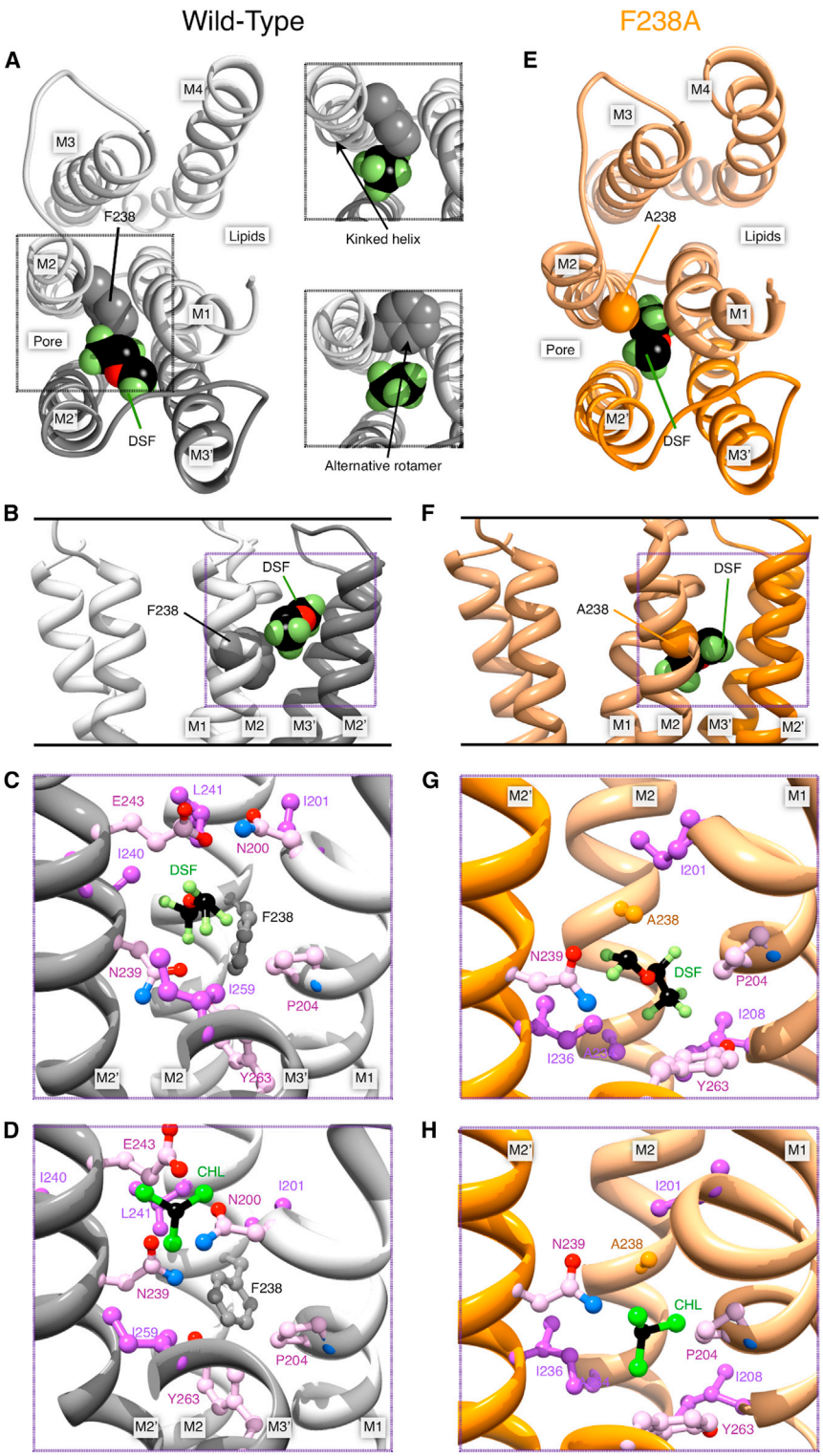

Figure 4. Desflurane and Chloroform Poses in the Intersubunit Cavity of GLIC

(A) Left, GLIC structure with desflurane in the intersubunit binding site, viewed from the extracellular side. For clarity, only M1–M4 of the upper subunit (light gray) and M2–M3 from the lower subunit (dark gray) are shown. F238 and helices contributing to the intrasubunit cavity are labeled. Right, forcing the ligand to bind in the WT close to F238 either induces a kink in M2 or requires F238 to adopt a different rotamer.

(B) Desflurane binding viewed in the plane of the membrane in the pore.

(C) Intersubunit environment for desflurane binding in WT GLIC; note the proximity to F238.

(D) Chloroform bound to the intersubunit site of WT GLIC.

(E–H) Corresponding illustrations for ligands bound to GLIC F238A. The mutation yields a much larger cavity for ligand binding between the subunits. In particular, in (G) and (H), desflurane and chloroform assume poses that would directly overlap with the F238 side chain.

See also Figures S1, S2, and Table S1.

an h-bond between T255 and desflurane, but nonpolar interactions with I202 and S205 and possibly polar interaction between desflurane and T255 (Figures 3C and 3G) because T255A reduces inhibition (Nury et al., 2011). No differences in these local interactions were observed between WT and F238A simulations.

Because the specific subsite for binding chloroform intrasubunit is not known from crystallographic structures, we tested three different subsites. One location was found close to Y254 and T255 in M3 as well as I201 and S205 in M1 (Figures 3D and 3E), which is identical to the binding site identified for desflurane. A second location involves I202 (M1), Y254 (M3), and N307 (M4), similar to the previously reported intrasubunit binding location for propofol (Nury et al., 2011). Finally, a third subsite involves V242, F238/A238, N239 (M2), and Y263 (M3). The latter is closer to the linking tunnel between intra- and intersubunit cavities and less exposed to the hydrophobic membrane region. Despite the small size and high mobility (rmsf values up to 2.83 Å) of chloroform, it stayed completely within these pockets during a 20 ns unrestrained simulation. Chloroform assumes three to four different orientations that convert rapidly and effectively behave as a single pose.

Intersubunit Binding Conformations

The intersubunit site is delimited by the M1, M2, M2′, and M3′ helices (with prime notation indicating the next subunit; Figure 4). We started our initial simulations with different poses for desflurane and chloroform. The locations of these ranged from deep into the TM domain close to the 14′ site to poses at the extracellular (EC)-TM interface of the inte-subunit cavity. For WT GLIC and F238A, we investigated a binding site for

Figure 5. Free Energy of Intra- versus Intersubunit Binding

Calculated affinities for GLIC WT (black) and F238A (orange) for desflurane and chloroform in both cavities (Table S2). SE estimates for the free energy calculation (see Supplemental Experimental Procedures) are indicated; **$p < 0.01$. Both ligands preferred intrasubunit binding in WT GLIC, but shift to primarily intersubunit binding in F238A. This correlates well with the functional results in Figure 1 and appears to suggest the intrasubunit binding site is primarily inhibitory while the intersubunit site is potentiating.

See also Figure S3.

desflurane close to the EC-TM interface (between N200 M1 and E243 M2′), similar to the site proposed for enflurane in GLIC (Chen et al., 2010). This part of the cavity is water-filled and made up by polar and charged residues N200, E243, K244, Y203, and S196 (Figure 2; Table S1). However, the binding free energies at this site turned out to be significantly higher than those at the intersubunit subsite close to the 14′ site. Furthermore, we expected structural changes caused by the 14′ mutation to be minimal at this site and not cause significant changes in anesthetic binding. Therefore, we mainly investigated the binding poses in proximity of the 14′ site, close to the linking tunnel between the intra- and intersubunit site (Figures 4B and 4F). This is the only site where changes were large enough to potentially explain the inversion of the anesthetic effect.

The binding site was defined by M2 A238, I243; M1 I201, P204, I208; M2′ R239, I240, I236; M3′ 263 and lined by N200 and E243. The rmsf of desflurane bound to WT GLIC was 1.86 Å and for the F238A mutant 1.99 Å. Furthermore, the two intersubunit conformations of desflurane in WT GLIC occupied the same pocket with two kinetically distinct orientations that only rarely interconverted, while the MD trajectories of the poses in the F238A mutant showed fast interchange between several conformations. Desflurane binding in WT GLIC is located more toward the EC domain, with a mass center roughly at the level of I240. There is no overlap with the corresponding binding locations of desflurane in the F238A mutant, where the site is roughly at the height of I236. This difference was mainly explained by the steric restriction caused by the F238 phenyl ring in WT GLIC (cf. Figures 4C and 4G), which also caused desflurane to bind closer to N200 and E243 in WT GLIC, where there is a water-filled polar cavity at the EC-TM interface. Consequently, the ether group of desflurane is not able to form polar interactions with N239 and Y263 or hydrophobic interactions with I236 and Y263 further down in the cavity. In contrast, desflurane bound to GLIC F238A resulted in just a single cluster representing one binding pose, where the ligand has characteristic polar interactions with M2′ N239 and M3′ Y263 and hydrophobic interactions with M3′ 263; M2′ I236, and M2 A238.

For chloroform in the intersubunit cavity, we identified a single site in WT GLIC with four slightly different conformations. As for desflurane, chloroform in the WT structure did not penetrate deeper than the level of I240 (16′) in M2′, which is significantly above the 14′ site. Three of the conformations identified were close to this 16′ site where they interact with N239 of M2′ (15′), and the last conformation close to N200 and E243 (similar to the desflurane binding in WT; Figure 4D). For chloroform too, there was a marked change of binding properties with the mutation. Chloroform binding to F238A GLIC had two kinetically distinct poses; the first is below the 14′ site close to I236 (M2′), A238 (M2) and the aromatic ring of Y263 (M3′), while the second pose is one helix turn further up at 16′ (I240 in M2′), forming polar contacts to N239 and Y263.

Binding Free Energies

The free energy of binding in each site was derived from MD simulations where ligands were restrained in each kinetically distinct orientation and interactions gradually decoupled (Wang et al., 2006). The free energy of binding for desflurane in the GLIC WT intrasubunit cavity was −21.8 ± 0.3 kJ/mol compared to −19.7 ± 0.4 kJ/mol for F238A (Figure 5). Importantly, these SE estimates only refer to the ligand sampling, not the much slower relaxation of the protein, which means the difference is likely not significant.

For the intrasubunit binding of chloroform, we calculated free energies in three different pockets. For the deeply buried pocket at the 14′ site close to V242, N239, and Y263, we retrieved a binding free energy of −3.9 ± 0.4 kJ/mol for WT and −4.1 ± 0.4 kJ/mol for the mutant. The chloroform sites that most closely resembled the propofol binding sites had binding free energies of −14.6 ± 0.3 kJ/mol for WT and −13.9 ± 0.4 kJ/mol for F238A. The intrasubunit chloroform site showing the strongest binding resulted in free energies of −18.6 ± 0.4 kJ/mol for WT and −15.5 ± 0.1 kJ/mol for F238A, which is closer to the binding affinity of desflurane. This reduction in affinity was not coupled to any change of pose, and further analysis indicated it is rather due to increased water penetration into the intrasubunit site, which as discussed previously by Howard and colleagues (Howard et al., 2011a) is a result of the increased volume of the intersubunit site in GLIC F238A (Table S1).

For binding between subunits, we first considered the higher-level site located closer to the EC domain. For desflurane binding in WT GLIC, the binding energy in this site was only −9.5 ± 0.4 kJ/mol, which was the worst of all scanned sites. Because this location is also relatively far from the 14′ site, we did not expect large changes from the F238A mutation and decided not to pursue this site further. To evaluate binding in the lower-level cavity (closer to 14′), the overall free energy of binding was obtained from occupancy-weighted averaging of the free energies of the multiple kinetically distinct poses. At the intersubunit 14′ site, the total free energy of desflurane binding was −14.4 ± 0.6 kJ/mol for WT GLIC and −23.2 ± 0.5 kJ/mol for the F238A mutant. Similarly, for chloroform, the free energy of binding in the intersubunit site was 16.2 ± 0.6 kJ/mol and −24.8 ± 0.3 kJ/mol for WT and F238A, respectively. Some caution is advised because protein relaxation could affect these

values on longer timescales, although we do not expect binding to *deteriorate* in the mutant with relaxation (which would be required to alter the qualitative result). The shifts in the intersubunit site are close to 10 kJ/mol, and even a relative difference of 5 kJ/mol corresponds to a factor ~10 in occupancy at room temperature. In other words, this suggests that the intrasubunit site is heavily favored for desflurane and favored for chloroform in WT GLIC, whereas the F238A mutation clearly shifts the most favorable location to the intersubunit site for both ligands (Table S2).

To test cooperativity between the two binding sites in F238A, we also calculated the free energies when desflurane was present in both binding sites. For the intrasubunit binding of desflurane, where desflurane was also present in the intersubunit, we obtain −20.9 ± 0.8 kJ/mol compared to −19.7 ± 0.4 kJ/mol without the extra ligand. The intersubunit site binding of desflurane with desflurane also present in the intrasubunit site was −23.9 ± 0.3 compared to −23.2 ± 0.5 kJ/mol for the reference case. Thus, it appears prior binding in one site has little influence on the affinity in the other site.

DISCUSSION

We previously showed that GLIC exhibits bimodal modulation by *n*-alcohols, being potentiated by short-chain alcohols (methanol, ethanol) but inhibited by long-chain alcohols (propanol and larger; Howard et al., 2011a). Substituting alanine for phenylalanine at the 14′ position in the GLIC M2 helix (F238A) dramatically altered alcohol modulation, enhancing potentiation by short-chain alcohols and converting alcohols as large as *n*-hexanol from inhibitors into potentiators (Howard et al., 2011a). The present work now shows that the F238A mutation also completely reverses the action of several volatile anesthetics, converting them from inhibitors into potentiators. Thus, consistent with past evidence that alcohols and anesthetics act via shared binding sites on pLGICs (Mascia et al., 2000), long-chain *n*-alcohols and anesthetics modulate GLIC in a parallel fashion, involving the F238 residue. Our free energy calculations on docked desflurane and chloroform suggest this is coupled to differential binding, with the intrasubunit site being preferred in WT GLIC, while the intersubunit site is enlarged and favored in the F238A mutant. We propose a model with two sites of action with opposing effects. The functional effect on the channel is a result of competitive binding between these two sites, although there does not appear to be any cooperativity effects between the sites. This could explain the complex dose-response curve where binding to a single site initially causes the effect, but when this is saturated and the second site is increasingly occupied, the effect is suddenly reversed. In contrast, a single site-model where occupancy triggers different modes of action would likely result in a linear dose-response curve.

Previous structural studies raised the possibility that the occupancy of anesthetics, even at saturating concentrations, might be low in GLIC TM cavities, given the high B-factors associated with the bound drugs (Nury et al., 2011). In contrast, our simulations are consistent with the explanation that high B-factors arise from high mobility and conformational entropy of the anesthetic molecule within its binding site: in many cases, the modulator was seen to flip its orientation 180° several times in the course of a single simulation. We were able to observe this mobility in all five semisymmetric cavities docked in each simulation, but with no evident cooperativity. This high mobility may arise from a lack of strong electrostatic interactions defining a particular pose in the binding cavity.

Assuming high overall occupancy, we infer that even relatively disfavored binding sites contribute to the net modulation, particularly under the high (low millimolar) concentrations of anesthetics used for functional experiments in this study. This hypothesis is consistent with previous studies supporting the existence of multiple simultaneous interaction sites for allosteric modulators on pLGICs, in some cases with opposing functional consequences (Borghese et al., 2003; Crawford et al., 2007; Howard et al., 2011b). Indeed, the low Hill coefficients observed for anesthetic inhibition of WT GLIC are consistent with multiple antagonistic sites of action or possibly with negative cooperativity (Weng et al., 2010). We also noted that, although high concentrations of desflurane dramatically potentiated GLIC F238A currents, moderate concentrations (<3 MAC) had a smaller absolute effect on the mutant than on WT: 1 MAC desflurane inhibited WT GLIC by 50%, but did not significantly alter GLIC F238A. This decreased apparent affinity is consistent with more closely balanced binding at opposing sites of action in the mutant, as predicted by our binding free energy calculations.

The intrasubunit cavity used for initial docking in this study was the unique site of desflurane binding in a recent crystal structure of WT GLIC (Nury et al., 2011). Of the three binding poses we identified for desflurane in WT GLIC, the highest affinity one was remarkably close to the X-ray co-crystal. Chloroform too was found to bind in this location, while the propofol site in the co-crystal is more similar to one of our alternative poses. Given that WT GLIC exhibits net inhibition by desflurane, this site was proposed to be an inhibitory site of action (Nury et al., 2011). Conversely, a nearby cavity at the intersubunit interface was recently implicated in potentiating actions of *n*-alcohols on GLIC (Howard et al., 2011a) as well as GlyRs (Murail et al., 2011). In this study, we provide quantitative measures of the relative free energies of binding to the intrasubunit (putative inhibitory) and intersubunit (putative potentiating) cavities in GLIC WT and F238A channels. The F238A mutation made desflurane binding to the intrasubunit site slightly less favorable, but enhanced binding to the intersubunit site 2-fold. The net effect implies there should be an inversion of the occupancy in the two sites, which correlates well with a switch from inhibition to potentiation by desflurane.

In the intersubunit cavity, we tested three possible docking poses at varying levels of penetration into the TM core. For the F238A mutant, the deepest binding pose—essentially occupying the cavity left by the substituted F238 side chain—was the most favorable. However, in the WT protein, this pose was almost completely occluded; instead, the optimal intersubunit pose was translated by one helical turn toward the extracellular medium, near residue L241. This binding pose is supported by our previous demonstration that small substitutions at residue 241 enhance ethanol potentiation and that labeling of this residue with a small methanethiosulfonate reagent mimics alcohol potentiation (Howard et al., 2011a). We tested an additional binding pose even further toward the EC space, but found it to be a less significant contributor to binding in either WT or mutant proteins.

The free energy calculations also indicate that desflurane binds with similar affinity to the intrasubunit and intersubunit cavities of the GLIC F238A mutant. Indeed, as discussed previously, moderate desflurane concentrations (1 MAC) have no net effect on GLIC F238A, possibly reflecting a balance of inhibiting and potentiating actions. Although one cannot directly translate affinity to efficacy, this might be reflected in the free energies where the difference between the two sites in F238A is much smaller for desflurane (one in four desfluranes would still occupy the inhibitory site) than chloroform (one in 50).

However, at high concentrations, desflurane is a strong potentiator of the GLIC F238A mutant. The net functional effect, then, may arise from a combination of inhibitory binding to the intrasubunit cavity, plus potentiating interactions with the intersubunit cavity that are of higher absolute efficacy. As the putative inhibitory effect of binding in the intrasubunit cavity saturates, binding to an intersubunit site with a relatively higher efficacy (but for potentiation rather than inhibition) could yield the strong net enhancement observed experimentally. This is in agreement with a multiple-site model for allosteric regulation. In the WT channel, the low affinity of binding in the intersubunit cavity may render it a negligible contributor to net modulation, except at very high concentrations not tolerated in our oocyte assay. Of course, it is also possible that structural changes brought by the F238A mutation increase the efficacy of intersubunit binding relative to WT, such that the increased affinity reflected in our free energy calculations leads to an even more dramatically increased potency of potentiation at high concentrations.

In addition to the intrasubunit and intersubunit TM cavities studied here, previous molecular dynamics studies (Brannigan et al., 2010; Chen et al., 2010) have implicated anesthetic binding sites near the channel pore and M2–M3 loop. Although our simulations provide a simple quantitative basis for our functional observations, there could be possible contributions from additional binding sites or possibly competitive effects from pore blocking (LeBard et al., 2012); some of this might be possible to test by combining free energy calculations of the two sites studied here with pore blocking to understand pLGIC modulation, although this might require an extension to the simplified two-site model. However, given the presumed promiscuity of anesthetic binding and their evidently high mobility within a given binding site, we defined the ''intrasubunit'' and ''intersubunit'' site for each protein as the most favorable of a variety of tested poses. Docking of desflurane in the intrasubunit cavity yielded a binding pose superimposable with that observed in the crystal structure (Nury et al., 2011). Docking in alternative poses in this WT cavity yielded less favorable energies. Furthermore, the intrasubunit binding pose observed for WT GLIC was conserved in the F238A structure, consistent with the comparable free energy of intrasubunit binding for the two proteins.

The binding of general anesthetics to GLIC is likely not limited to the intrasubunit (I202, S205, and T255) and the intersubunit (N239, Y263, and I236) sites. A binding site close to the TM domain/EC domain interface reported for halothane and thiopental above N200 (Chen et al., 2010) might also be suitable for polar anesthetics. Despite lower affinity, we too observed a possible binding pose for desflurane in this location in WT GLIC, and ethanol modulation of GLIC was also somewhat affected by alterations to I240, L241, or N245.

Phenylalanine is conserved at the M2 14′ position of several subtypes of nAChRs, which—like GLIC—were previously shown to exhibit potentiation by short-chain alcohols but inhibition by anesthetics and long-chain alcohols (Borghese et al., 2003). Conversely, the equivalent residue is generally smaller and more polar in channels such as $GABA_A$Rs and GlyRs, which exhibit potentiation rather than inhibition by anesthetics and alcohols. The recently crystallized GluClα has a glutamine in this position, and the co-crystal with the potentiator ivermectin shows the large ligand to be placed between subunits (Hibbs and Gouaux, 2011), overlapping with our highest-affinity site for anesthetics in GLIC F238A.

The effect of substituting a smaller, more polar residue at the 14′ position in GLIC is thus consistent with a role for this position, and the nearby intersubunit cavity, in differential sensitivity of pLGICs to allosteric modulators. Previous studies on GlyR and $GABA_A$R linked several residues belonging to different subunits to the modulation of anesthetics and alcohols, which supports functional effects between subunits, in particular the 15′ residues α_1S270/β_2N265 (15′ M2) of $GABA_A$R (Mihic et al., 1997) and S267 (15′ M2) of GlyR or S260 (15′ M2) of GluCl (Cheng et al., 2008). These sites are very close to the 14′ site in the present study and support a general anesthetic- and alcohol-binding site in this location, which appears to be confirmed by a recent GLIC F238A co-crystal with ethanol bound intersubunit (Sauguet et al., 2013). Similarly, the earlier structure of GLIC in a locally closed state (Prevost et al., 2012) indicates that the extracellular part of M2 helix has moved inward, to some extent detached from M3, and opened a cavity between them. Our intrasubunit site is located close to the lower part of this cavity, and it appears quite reasonable that ligand binding in this site could stabilize an already closed channel, resulting in the observed inhibition, while potentiation in GLIC F238A might be caused by subunits not being able to move inward when ligands are bound between them.

In addition to the binding interactions studied here, there may be indirect effects of the F238A mutation on modulation due to changes in the energetics of gating. As described previously, the mutation did right-shift the proton concentration dependence, adjusting the 10% activation condition from pH 5.5 to pH 5.0; however, neighboring mutations that elicited similar shifts in gating (e.g., A237C, N239C) did not evoke similar changes in alcohol modulation, suggesting that these effects were independent (Howard et al., 2011a). It should also be noted that our structural models are based on the crystallographic, presumed open (Bocquet et al., 2009; Hilf et al., 2010) or desensitized (Gonzalez-Gutierrez and Grosman, 2010; Parikh et al., 2011) state of GLIC. The pore radius did not change significantly during the short timescale of our simulations (Figure S2), which is not surprising because closing, desensitizing, or opening are likely much slower transitions. A complete understanding of the impact of modulator binding in the sites studied here or elsewhere will require a detailed model of the channel's opening and closing transitions, including the relative free energies of the channel in (future) closed versus open states and the transition states between them. However, better understanding of anesthetic binding in the intersubunit site is an important step toward understanding modulation of ligand-gated channels in general.

 ©2013 Elsevier Ltd All rights reserved

EXPERIMENTAL PROCEDURES

Experimental Materials

Volatile anesthetics were purchased from Marsam Pharmaceuticals Inc. (Cherry Hill, NJ); all other chemicals were purchased from Sigma-Aldrich (St. Louis, MO). Expression plasmids containing GLIC WT and F238A cDNA in the PMT3 vector were prepared as previously described (Howard et al., 2011a). The oocytes were prepared from ovarian tissue of *Xenopus laevis* frogs for the two-electrode voltage clamp electrophysiology. Procedures involving frogs were approved by the University of Texas at Austin Institutional Animal Care and Use Committee. GLIC currents were measured for pH-dependent GLIC activation as previously described (Howard et al., 2011a; see Supplemental Experimental Procedures for additional details).

Volatile anesthetic solutions were adjusted to deliver the reported concentration calibrated by gas chromatography, as described previously (Lin et al., 1992). The adjusted anesthetic volume was added via positive displacement pipette to the appropriate Ringer's buffer in a scintillation vial with minimal head space, immediately sealed with parafilm and aluminum foil, and sonicated for $\geq$ 2 min. The solution was applied by piercing the seal with the perfusion input needle, minimizing exposure of the solution surface to atmosphere. To quantify anesthetic modulation, oocytes were treated for 1 min with low-pH Ringer's buffer; after 5 min washout, the anesthetic solution was applied in neutral Ringer's buffer for 1 min, then in low-pH buffer for 1 min; after another 5 min washout, low-pH buffer was again applied alone. Modulation was calculated as $[(R_A - < R_0,R_1 >) / < R_0,R_1 >] \times 100$, where R_A represents the channel response in the presence of anesthetic and $< R_0,R_1 >$ represents the mean of the pre- and postanesthetic responses. Initial anesthetic concentrations were chosen as three times MAC, except for chloroform, for which ~1 MAC was used on account of the large degree of modulation. Values of MAC were derived as previously described (Mihic et al., 1994).

Statistics

Data are represented as mean ± SEM. Results were analyzed by two-tailed unpaired t test with significance set at $p < 0.05$. The desflurane inhibition curve for WT GLIC was calculated by nonlinear regression fit to the equation $M = 100 / (1 + 10^{\wedge}[\log(IC_{50} - A)] \cdot n_H) - 100$, where M is the percentage modulation, A is the molar concentration of desflurane, IC_{50} is the concentration producing 50% inhibition, and n_H is the Hill coefficient. Nonlinear regression analysis and all statistical analyses were performed with GraphPad Prism 5 for Mac (GraphPad Software, San Diego, CA).

Molecular Modeling

Protein Data Bank ID code 3EAM (Bocquet et al., 2009) was used for WT GLIC. Both WT and F238A systems were embedded into a DOPC bilayer, solvated, and set to a 100 mM concentration of NaCl (Howard et al., 2011a). Both systems were subject to 20 ns of simulation with position restraints on backbone atoms, and the mutant relaxed another 200 ns. Initial ligand poses were identified with AutoDock 4.2 (Morris et al., 1998) and subject to 20 ns unrestrained simulations with GROMACS (Hess et al., 2008) to get the kinetically distinct ligand binding poses. A restraining potential was used during free energy calculations (Figure S3). Additional details about docking and parameters are described in the Supplemental Experimental Procedures.

SUPPLEMENTAL INFORMATION

Supplemental Information includes Supplemental Experimental Procedures, three figures, and two tables and can be found with this article online at http://dx.doi.org/10.1016/j.str.2013.06.018.

ACKNOWLEDGMENTS

This work was supported by the European Research Council (209825), the Foundation for Strategic Research, the Swedish Research Council (2010-491, 2010-5107), the Swedish e-Science Research Center, and National Institutes of Health/National Institutes on Alcohol Abuse and Alcoholism grants T32 AA007471, R01 AA06399, and R01 AA013378. Computational resources were provided by the Swedish National Infrastructure for Computing.

Received: February 12, 2013
Revised: June 8, 2013
Accepted: June 13, 2013
Published: July 25, 2013

REFERENCES

Arevalo, E., Chiara, D.C., Forman, S.A., Cohen, J.B., and Miller, K.W. (2005). Gating-enhanced accessibility of hydrophobic sites within the transmembrane region of the nicotinic acetylcholine receptor's delta-subunit. A time-resolved photolabeling study. J. Biol. Chem. *280*, 13631–13640.

Bali, M., and Akabas, M.H. (2004). Defining the propofol binding site location on the GABAA receptor. Mol. Pharmacol. *65*, 68–76.

Bertaccini, E.J., Shapiro, J., Brutlag, D.L., and Trudell, J.R. (2005). Homology modeling of a human glycine alpha 1 receptor reveals a plausible anesthetic binding site. J. Chem. Inf. Model. *45*, 128–135.

Bocquet, N., Prado de Carvalho, L., Cartaud, J., Neyton, J., Le Poupon, C., Taly, A., Grutter, T., Changeux, J.P., and Corringer, P.J. (2007). A prokaryotic proton-gated ion channel from the nicotinic acetylcholine receptor family. Nature *445*, 116–119.

Bocquet, N., Nury, H., Baaden, M., Le Poupon, C., Changeux, J.P., Delarue, M., and Corringer, P.J. (2009). X-ray structure of a pentameric ligand-gated ion channel in an apparently open conformation. Nature *457*, 111–114.

Borghese, C.M., Henderson, L.A., Bleck, V., Trudell, J.R., and Harris, R.A. (2003). Sites of excitatory and inhibitory actions of alcohols on neuronal alpha2beta4 nicotinic acetylcholine receptors. J. Pharmacol. Exp. Ther. *307*, 42–52.

Brannigan, G., LeBard, D.N., Hénin, J., Eckenhoff, R.G., and Klein, M.L. (2010). Multiple binding sites for the general anesthetic isoflurane identified in the nicotinic acetylcholine receptor transmembrane domain. Proc. Natl. Acad. Sci. USA *107*, 14122–14127.

Brejc, K., van Dijk, W.J., Klaassen, R.V., Schuurmans, M., van Der Oost, J., Smit, A.B., and Sixma, T.K. (2001). Crystal structure of an ACh-binding protein reveals the ligand-binding domain of nicotinic receptors. Nature *411*, 269–276.

Cascio, M. (2006). Modulating inhibitory ligand-gated ion channels. AAPS J. *8*, E353–E361.

Chen, Q., Cheng, M.H., Xu, Y., and Tang, P. (2010). Anesthetic binding in a pentameric ligand-gated ion channel: GLIC. Biophys. J. *99*, 1801–1809.

Cheng, M.H., Coalson, R.D., and Cascio, M. (2008). Molecular dynamics simulations of ethanol binding to the transmembrane domain of the glycine receptor: implications for the channel potentiation mechanism. Proteins *71*, 972–981.

Chiara, D.C., Dangott, L.J., Eckenhoff, R.G., and Cohen, J.B. (2003). Identification of nicotinic acetylcholine receptor amino acids photolabeled by the volatile anesthetic halothane. Biochemistry *42*, 13457–13467.

Chiara, D.C., Hamouda, A.K., Ziebell, M.R., Mejia, L.A., Garcia, G., 3rd, and Cohen, J.B. (2009). [(3)H]chlorpromazine photolabeling of the torpedo nicotinic acetylcholine receptor identifies two state-dependent binding sites in the ion channel. Biochemistry *48*, 10066–10077.

Chiara, D.C., Dostalova, Z., Jayakar, S.S., Zhou, X., Miller, K.W., and Cohen, J.B. (2012). Mapping general anesthetic binding site(s) in human $\alpha1\beta3$ γ-aminobutyric acid type A receptors with [^{3}H]TDBzl-etomidate, a photoreactive etomidate analogue. Biochemistry *51*, 836–847.

Corringer, P.J., Poitevin, F., Prevost, M.S., Sauguet, L., Delarue, M., and Changeux, J.P. (2012). Structure and pharmacology of pentameric receptor channels: from bacteria to brain. Structure *20*, 941–956.

Crawford, D.K., Trudell, J.R., Bertaccini, E.J., Li, K.X., Davies, D.L., and Alkana, R.L. (2007). Evidence that ethanol acts on a target in Loop 2 of the extracellular domain of alpha1 glycine receptors. J. Neurochem. *102*, 2097–2109.

Duret, G., Van Renterghem, C., Weng, Y., Prevost, M., Moraga-Cid, G., Huon, C., Sonner, J.M., and Corringer, P.J. (2011). Functional prokaryotic-eukaryotic chimera from the pentameric ligand-gated ion channel family. Proc. Natl. Acad. Sci. USA *108*, 12143–12148.

Ernst, M., Bruckner, S., Boresch, S., and Sieghart, W. (2005). Comparative models of GABAA receptor extracellular and transmembrane domains: important insights in pharmacology and function. Mol. Pharmacol. *68*, 1291–1300.

Foloppe, N., and Hubbard, R. (2006). Towards predictive ligand design with free-energy based computational methods? Curr. Med. Chem. *13*, 3583–3608.

Forman, S.A., and Miller, K.W. (2011). Anesthetic sites and allosteric mechanisms of action on Cys-loop ligand-gated ion channels. Can. J. Anaesth. *58*, 191–205.

Gonzalez-Gutierrez, G., and Grosman, C. (2010). Bridging the gap between structural models of nicotinic receptor superfamily ion channels and their corresponding functional states. J. Mol. Biol. *403*, 693–705.

Hess, B., Kutzner, C., van der Spoel, D., and Lindahl, E. (2008). GROMACS 4: algorithms for highly efficient, load-balanced, and scalable molecular simulation. J. Chem. Theory Comput. *4*, 435–447.

Hibbs, R.E., and Gouaux, E. (2011). Principles of activation and permeation in an anion-selective Cys-loop receptor. Nature *474*, 54–60.

Hilf, R.J., Bertozzi, C., Zimmermann, I., Reiter, A., Trauner, D., and Dutzler, R. (2010). Structural basis of open channel block in a prokaryotic pentameric ligand-gated ion channel. Nat. Struct. Mol. Biol. *17*, 1330–1336.

Howard, R.J., Murail, S., Ondricek, K.E., Corringer, P.J., Lindahl, E., Trudell, J.R., and Harris, R.A. (2011a). Structural basis for alcohol modulation of a pentameric ligand-gated ion channel. Proc. Natl. Acad. Sci. USA *108*, 12149–12154.

Howard, R.J., Slesinger, P.A., Davies, D.L., Das, J., Trudell, J.R., and Harris, R.A. (2011b). Alcohol-binding sites in distinct brain proteins: the quest for atomic level resolution. Alcohol. Clin. Exp. Res. *35*, 1561–1573.

Jansen, M., and Akabas, M.H. (2006). State-dependent cross-linking of the M2 and M3 segments: functional basis for the alignment of GABAA and acetylcholine receptor M3 segments. J. Neurosci. *26*, 4492–4499.

Laskowski, R.A. (1995). SURFNET: a program for visualizing molecular surfaces, cavities, and intermolecular interactions. J. Mol. Graph. *13*, 323–330, 307–328.

LeBard, D.N., Hénin, J., Eckenhoff, R.G., Klein, M.L., and Brannigan, G. (2012). General anesthetics predicted to block the GLIC pore with micromolar affinity. PLoS Comput. Biol. *8*, e1002532.

Li, G.D., Chiara, D.C., Sawyer, G.W., Husain, S.S., Olsen, R.W., and Cohen, J.B. (2006). Identification of a GABAA receptor anesthetic binding site at subunit interfaces by photolabeling with an etomidate analog. J. Neurosci. *26*, 11599–11605.

Lin, L.H., Chen, L.L., Zirrolli, J.A., and Harris, R.A. (1992). General anesthetics potentiate gamma-aminobutyric acid actions on gamma-aminobutyric acidA receptors expressed by Xenopus oocytes: lack of involvement of intracellular calcium. J. Pharmacol. Exp. Ther. *263*, 569–578.

Lindahl, E., and Sansom, M.S. (2008). Membrane proteins: molecular dynamics simulations. Curr. Opin. Struct. Biol. *18*, 425–431.

Mascia, M.P., Trudell, J.R., and Harris, R.A. (2000). Specific binding sites for alcohols and anesthetics on ligand-gated ion channels. Proc. Natl. Acad. Sci. USA *97*, 9305–9310.

Meyer, T. (2010). Managing inhaled anesthesia: challenges from a health-system pharmacist's perspective. Am. J. Health Syst. Pharm. *67*(8, Suppl 4), S4–S8.

Mihic, S.J., McQuilkin, S.J., Eger, E.I., 2nd, Ionescu, P., and Harris, R.A. (1994). Potentiation of gamma-aminobutyric acid type A receptor-mediated chloride currents by novel halogenated compounds correlates with their abilities to induce general anesthesia. Mol. Pharmacol. *46*, 851–857.

Mihic, S.J., Ye, Q., Wick, M.J., Koltchine, V.V., Krasowski, M.D., Finn, S.E., Mascia, M.P., Valenzuela, C.F., Hanson, K.K., Greenblatt, E.P., et al. (1997). Sites of alcohol and volatile anaesthetic action on GABA(A) and glycine receptors. Nature *389*, 385–389.

Miller, K.W. (2002). The nature of sites of general anaesthetic action. Br. J. Anaesth. *89*, 17–31.

Morris, G.M., Goodsell, D.S., Halliday, R.S., Huey, R., Hart, W.E., Belew, R.K., and Olson, A.J. (1998). Automated docking using a Lamarckian genetic algorithm and an empirical binding free energy function. J. Comput. Chem. *19*, 1639–1662.

Mowrey, D., Cheng, M.H., Liu, L.T., Willenbring, D., Lu, X., Wymore, T., Xu, Y., and Tang, P. (2013). Asymmetric ligand binding facilitates conformational transitions in pentameric ligand-gated ion channels. J. Am. Chem. Soc. *135*, 2172–2180.

Murail, S., Wallner, B., Trudell, J.R., Bertaccini, E., and Lindahl, E. (2011). Microsecond simulations indicate that ethanol binds between subunits and could stabilize an open-state model of a glycine receptor. Biophys. J. *100*, 1642–1650.

Murail, S., Howard, R.J., Broemstrup, T., Bertaccini, E.J., Harris, R.A., Trudell, J.R., and Lindahl, E. (2012). Molecular mechanism for the dual alcohol modulation of Cys-loop receptors. PLoS Comput. Biol. *8*, e1002710.

Nury, H., Van Renterghem, C., Weng, Y., Tran, A., Baaden, M., Dufresne, V., Changeux, J.P., Sonner, J.M., Delarue, M., and Corringer, P.J. (2011). X-ray structures of general anaesthetics bound to a pentameric ligand-gated ion channel. Nature *469*, 428–431.

Pandhare, A., Hamouda, A.K., Staggs, B., Aggarwal, S., Duddempudi, P.K., Lever, J.R., Lapinsky, D.J., Jansen, M., Cohen, J.B., and Blanton, M.P. (2012). Bupropion binds to two sites in the Torpedo nicotinic acetylcholine receptor transmembrane domain: a photoaffinity labeling study with the bupropion analogue [(125)I]-SADU-3-72. Biochemistry *51*, 2425–2435.

Parikh, R.B., Bali, M., and Akabas, M.H. (2011). Structure of the M2 transmembrane segment of GLIC, a prokaryotic Cys loop receptor homologue from Gloeobacter violaceus, probed by substituted cysteine accessibility. J. Biol. Chem. *286*, 14098–14109.

Pedersen, S.E., and Cohen, J.B. (1990). d-Tubocurarine binding sites are located at alpha-gamma and alpha-delta subunit interfaces of the nicotinic acetylcholine receptor. Proc. Natl. Acad. Sci. USA *87*, 2785–2789.

Perkins, D.I., Trudell, J.R., Crawford, D.K., Alkana, R.L., and Davies, D.L. (2010). Molecular targets and mechanisms for ethanol action in glycine receptors. Pharmacol. Ther. *127*, 53–65.

Pettersen, E.F., Goddard, T.D., Huang, C.C., Couch, G.S., Greenblatt, D.M., Meng, E.C., and Ferrin, T.E. (2004). UCSF Chimera—a visualization system for exploratory research and analysis. J. Comput. Chem. *25*, 1605–1612.

Prevost, M.S., Sauguet, L., Nury, H., Van Renterghem, C., Huon, C., Poitevin, F., Baaden, M., Delarue, M., and Corringer, P.J. (2012). A locally closed conformation of a bacterial pentameric proton-gated ion channel. Nat. Struct. Mol. Biol. *19*, 642–649.

Sauguet, L., Howard, R.J., Malherbe, L., Lee, U.S., Corringer, P.J., Harris, R.A., and Delarue, M. (2013). Structural basis for potentiation by alcohols and anaesthetics in a ligand-gated ion channel. Nat Commun *4*, 1697.

Sonner, J.M., Antognini, J.F., Dutton, R.C., Flood, P., Gray, A.T., Harris, R.A., Homanics, G.E., Kendig, J., Orser, B., Raines, D.E., et al. (2003). Inhaled anesthetics and immobility: mechanisms, mysteries, and minimum alveolar anesthetic concentration. Anesth. Analg. *97*, 718–740.

Trudell, J.R., and Bertaccini, E. (2004). Comparative modeling of a GABAA alpha1 receptor using three crystal structures as templates. J. Mol. Graph. Model. *23*, 39–49.

Unwin, N. (2005). Refined structure of the nicotinic acetylcholine receptor at 4A resolution. J. Mol. Biol. *346*, 967–989.

Urban, B.W., and Bleckwenn, M. (2002). Concepts and correlations relevant to general anaesthesia. Br. J. Anaesth. *89*, 3–16.

Wang, J., Deng, Y., and Roux, B. (2006). Absolute binding free energy calculations using molecular dynamics simulations with restraining potentials. Biophys. J. *91*, 2798–2814.

Weng, Y., Yang, L.Y., Corringer, P.J., and Sonner, J.M. (2010). Anesthetic sensitivity of the Gloeobacter violaceus proton-gated ion channel. Anesth. Analg. *110*, 59–63.

Yamodo, I.H., Chiara, D.C., Cohen, J.B., and Miller, K.W. (2010). Conformational changes in the nicotinic acetylcholine receptor during gating and desensitization. Biochemistry *49*, 156–165.

Ziebell, M.R., Nirthanan, S., Husain, S.S., Miller, K.W., and Cohen, J.B. (2004). Identification of binding sites in the nicotinic acetylcholine receptor for [3H] azietomidate, a photoactivatable general anesthetic. J. Biol. Chem. *279*, 17640–17649.

 ©2013 Elsevier Ltd All rights reserved